NÖHÜ Müh. Bilim. Derg. / NOHU J. Eng. Sci., 2023; 12(4), 1621-1629

Niğde Ömer Halisdemir Üniversitesi Mühendislik Bilimleri Dergisi
Niğde Ömer Halisdemir University Journal of Engineering Sciences

Araştırma makalesi / Research article

www.dergipark.org.tr/tr/pub/ngumuh / www.dergipark.org.tr/en/pub/ngumuh

Modeling of carbon dioxide electrolysis with reversible fuel cells

Tersinir yakıt hücreleri ile karbondioksit elektrolizinin modellenmesi

Hasan Özcan[1,*]

[1] *Ankara Yıldırım Beyazıt University, Department of Mechanical Engineering, 06220, Ankara, Türkiye*

Abstract

In this study use of a reversible solid oxide fuel cell for co-electrolysis of steam and carbon dioxide is investigated using zero and multi-dimensional modeling tools. A zero-dimensional model is taken into account as the base model and applied to a single-cell system. Dimensions of the cell is used for the zero-dimensional model to provide a base for the multi-dimensional performance enhancement of the cell at micro to macro scales. An optimal current density is available at slightly lower than 1000 A/m^2 to provide low overpotentials and higher efficiency. Maximum reachable cell efficiency in this case is about 75%.

Keywords: Co-electrolysis, Reversible fuel cells, Carbon dioxide

Öz

Bu çalışmada sıfır ve çok boyutlu modelleme araçları ile tersinir bir yakıt hücresinde buhar ve karbon dioksit elektrolizi incelenmiştir. Temel alınan modeli olşuturmak için sıfır boyutlu bir model göz önüne alınmış ve sonuçlar tekli bir hücreye uygulanmıştır. Varolan hücrenin boyutları sıfır boyutlu modelde kullanılarak doğrulama yapılmış ve mikro ve makro ölçekte çok boyutlu performans arttırımı için temel oluşturmuştur. Optimum akım yoğunluğu olan 1 kA/m^2 değerinde düşük aşırı gerilim değerleri ede edilmiş ve yüksek verimlilik sağlanmıştır. Ulaşılabilir en yüksek verim %75 olarak gözlemlenmiştir.

Anahtar kelimeler: İkili elektroliz, Tersinir yakıt hücresi, Karbondioksit

1 Introduction

High temperature reversible fuel cells known as Solid oxide electrolysis cells (SOEC) or High temperature steam electrolysis (HTSE) are known as promising and effective solutions for a low carbon economy which utilizes electricity and high temperature heat to generate hydrogen from water. SOEC technology can also be used to electrolyze water/CO_2 mixtures from various sources for chemical feedstock production mainly called as syngas.

High temperature co-electrolysis (HTCE) of H_2O/CO_2 is reported as an efficient and a near/long-term cost-effective method, being more energy efficient than separate electrolysis of H_2O and CO_2. The syngas produced can be used as an energy carrier as well as in large scale energy storage [1-3]. This technology can offer an attractive route to decrease CO_2 emissions and facilitate integration of renewable energy technologies [4-7]. For the technology to be feasible enough for operation, some main targets are to be reached such as compatibility, flexibility, adaptability and affordability. Therefore, research is focused on longer life operation for cost-competitiveness with studies being conducted on electrode, cell sealing, electrolyte materials in cell and stack level, balance-of-plant components, and thermal-electrical integration of the processes [8].

Material requirements for the HTSE/HTCE technology have been designated to be high conductivity, compatible thermal expansion, dimensional, thermomechanical, and chemical stability of electrodes; chemically stable interconnect and sealing materials to prevent poisoning, and optimal electronic and ionic conduction of electrolyte for lower overpotentials through operation [9-13]. Some fuel electrode materials that have been used for HTCE operation are Ni-YSZ, LSV and LSCM while $CaTiO_3$, LSM, LSCF, LSCM-Cu metal-metal, ceramic-metal electrodes are used for the oxygen electrode [14-16]. Some issues with electrode materials can be listed as follows:

- Costly noble metals
- Ni has a thermal mismatch to SZ
- Catalytic properties and stabilities of ceramic electrodes are not optional
- Delamination between oxygen electrode and electrolyte (Some studies are present claiming cycling between SOEC/SOFC mode cures delamination [17-19])
- Cr, B, S, SiO_2 poisoning
- Redox of Ni catalyst causes volume changes in the fuel electrode causing mechanical stresses
- High steam partial pressure and high current density cause formation of a Ni layer on the fuel electrode surface, blocking oxygen transfer [20,21]

Above issues cause degradation, resulting in shorter plant life and higher product costs. Therefore, a major amount of research is focused on degradation studies [22-30]. However, some recent studies show that degradation is decreased down to 1.7-6 % per 1000 hours by altering operational conditions and modifying cell architecture [31-33].

Some institutes working on HTCE technologies are listed below:

- Idaho National Laboratories (INL) [34-36]: Feasibility of HTCEs with SOEC technology.

* Sorumlu yazar / Corresponding author, e-posta / e-mail: h.ozcan@aybu.edu.tr (H. Özcan)
Geliş / Recieved: 14.09.2023 Kabul / Accepted: 03.10.2023 Yayımlanma / Published: 15.10.2023
doi: 10.28948/ngmuh.1360333

- Northwestern University [37]: Renewables to liquids process with HTCE
- Columbia University [38]: HTCE for sustainable hydrocarbon fuels
- University of South Carolina [39]: Novel electrode materials for HTCE, Combining HTCE and methane partial oxidation
- Riso National Laboratory (RNL): Degradation of SOEC under HTCE mode, Large scale CH_4 and CO_2 storage with HTCEs [40].

Many other institutions conduct research on HTSE technology for water electrolysis. There are also numerous studies reporting efficiencies, thermal systems integration, topical thermodynamic and economic analysis as well as electrochemical models of HTCE technologies. Some recent studies can be found elsewhere [41-45]. There has been little work related to CO_2 activation process through the stack and diversion between reverse water gas shift reaction and electrolysis for CO production. Research is mainly focused on material/chemistry science of the cell to decrease delamination on oxygen electrodes, decreased cell poisoning, and novel electrode materials for increased life span of HTCE stack. Some studies are carried out for large-scale applications and connection of the HTCE to renewables to improve economic and technological feasibility for practical implementation for sustainable fuels. There is also limited work on electrical energy storage with HTCE technology. Limited number of studies are conducted for integrating HTCE technology to synthetic fuel reactors for liquid fuels production such as Fischer-Tropsch synthesis or other processes for methane, methanol etc. production. Just a couple transient heat-up, start-up models are present for only SOFC mode while there are no available studies for HTSE or HTCE [46]. There are no numerical investigations for effects of thermal expansion in electrodes or thermomechanical stresses on degradation or HTCE operation. There are not enough comprehensive studies made for 1-3D models to study HTCE in cell/stack level under variable operation conditions.

In this paper, a zero-dimensional model is considered as a base model and applied to a single cell system. Dimensions of the single cell is used for the zero-dimensional model to provide a base for the multi-dimensional performance enhancement of the cell with micro to macro scales. Multi-dimensional analysis of the cell is conducted by forming necessary geometric conditions using the COMSOL software package. The main motivation of the research is to model HTCE performance to potentially investigate a more efficient and cost-effective option that can be used as one of the unique technologies for carbon dioxide utilization.

2 Analysis and modeling

2.1 Zero-dimensional modeling

A zero-dimensional model of the HTCE system is initially developed utilizing existing analytical and experimental data. To initiate the electrochemical model, basic chemistry inside the cell is taken into account. The main chemical balance is as follows:

$$H_2O + CO_2 \rightarrow H_2 + CO + O_2 \quad (1)$$

Here, H_2O, CO_2, H_2 and CO are in gas mixture form at the cathode while O_2 is evolved on the anode side. The half-cell reactions are [47]:

$$2e^- + H_2O \rightarrow H_2 + O^{2-} \quad (2)$$

$$e^- + CO_2 \rightarrow CO + O^{2-} \quad (3)$$

There is also reverse water gas shift reaction occurring at certain cell temperatures as:

$$CO_2 + H_2 \rightarrow CO + H_2O \quad (4)$$

The open cell potential can be described as a function of cell potential where equilibrium compositions are used to determine the equation. The overall shift reaction occurs during the heat up:

$$y_{0,CO}CO + y_{0,CO_2}CO_2 + y_{0,H_2}H_2 + y_{0,H_2O}H_2O \rightarrow y_{1,CO}CO + y_{1,CO_2}CO_2 + y_{1,H_2}H_2 + y_{1,H_2O}H_2O \quad (5)$$

Here subscripts 0 represent cold inlets' molar flow rates while 1 refers to hot outlet before electrolysis. Corresponding balance equations for C, H and O are as follows:

$$y_{0,CO} + y_{0,CO2} = y_{1,CO} + y_{1,CO2} \quad (6)$$

$$y_{0,H_2} + y_{0,H_2O} = y_{1,H_2} + y_{1,H_2O} \quad (7)$$

$$y_{0,CO} + y_{0,CO2} + y_{0,H_2O} = y_{1,CO} + y_{1,CO2} + y_{1,H_2O} \quad (8)$$

Finally, the equilibrium constant for the shift reaction is:

$$K_{eq}(T) = \frac{y_{1,CO2}y_{1,H2}}{y_{1,CO}y_{1,H_2O}} \quad (9)$$

where,

$$\ln(K_{eq}) = \frac{4.92194x10^{-3}}{T} - 7.78386x10^{-1}\ln(T) + 2.5559x10^{-3}T - 5.0983x10^{-7}T^2 - 1.24911 \quad (10)$$

Above equations complete a set of four equations with four unknowns which results in determination of equilibrium composition before electrolysis. With the known equilibrium composition, the Nernst potential can be calculated using the known molar fractions [48]:

$$E_N = \frac{1}{y_{1,CO2} + y_{1,H_2O}} \langle y_{1,H_2O} \left\{ \frac{-\Delta G_{H_2O}}{2F} - \frac{\bar{R}T}{2F} \, ln \left[\frac{y_{1,H_2O}}{y_{1,H_2} y_{1,O_2}^{0.5}} \left(\frac{p}{p_{std}} \right)^{-0.5} \right] \right\} + y_{1,CO_2} \left\{ \frac{-\Delta G_{CO_2}}{2F} - \frac{\bar{R}T}{2F} \, ln \left[\frac{y_{1,CO_2}}{y_{1,CO} y_{1,O_2}^{0.5}} \left(\frac{p}{p_{std}} \right)^{-0.5} \right] \right\} \rangle \quad (11)$$

Here y_{O_2} is the mole fraction of oxygen in air and assumed as 0.21. In a similar way, electrolysis cell outlet equilibrium composition can be calculated by considering the electrochemical reduction. It should be noted that $\bar{R}$ is the molar universal gas constant, T is cell temperature, F is Faraday's constant and ΔG is the Gibbs free energy of the reaction. Therefore, oxygen evolution at anode should be included in the balance equation and it becomes:

$$y_{1,CO} + y_{1,CO2} + y_{1,H_2O} = y_{2,CO} + y_{2,CO2} + y_{2,H_2O} + \Delta n_o \quad (12)$$

Here, Δn_o is the relative molar rate of oxygen:

$$\Delta n_o = \frac{I_e}{2F\dot{N}_{tot}} \quad (13)$$

Where I_e is the total ionic current and $\dot{N}_{tot}$ the total molar flow rate at cathode inlet. Applying necessary balance equations, it is now possible to calculate the amount of syngas produced, power consumed and thermal efficiency of the cell. It should be noted that the minimum required inlet steam and CO_2 molar flow rates should satisfy the following constraint to prevent oxygen starvation in the cell:

$$\dot{N}_{H_2O} + \dot{N}_{CO_2} \geq \frac{I_e}{2F} \quad (14)$$

After securing the calculation of equilibrium gas composition, it is required to determine the total potential of the cell by considering overpotentials. Total cell potential is sum of the Nernst potential and corresponding overpotentials as follows:

$$E_{tot} = E_N + E_{con} + E_{act} + E_{ohm} \quad (15)$$

Where subscripts *con*, *act*, and *ohm* correspond to concentration, activation and ohmic. Activation overpotential is due to the chemical equilibrium state of ions at the electrode-electrolyte interface and due to overcoming of the electrical field occurring through transfer of charged particles. Butler-Volmer equation is generally utilized to determine activation overpotential:

$$j = j_{0,i} \left[\exp\left(\frac{\alpha z F E_{act,i}}{RT}\right) - exp \left[\frac{\left(-(1-\alpha) z F E_{act,i}\right)}{RT} \right] \right] \quad (16)$$

Where j is current density, j_0 is exchange current density, α is charge transfer coefficient, z is number of transferred electrons, and i represents anode or cathode. When the charge transfer coefficient is 0.5, Butler-Volmer equation takes the following form:

$$j = 2j_{0,i} \sinh\left(\frac{F E_{act,i}}{zRT}\right) \quad (17)$$

Exchange current density can be evaluated as a function of activation energy of each electrode:

$$j_{0,i} = \gamma_i \exp\left(-\frac{E_i}{RT}\right) \quad (18)$$

Where E_i is activation energy for each electrode and γ is pre-exponential factor. Ohmic overpotentials are results of ionic, electronic, and contact resistances which can be given in a general form:

$$E_{ohm} = j \sum \ddot{R}_i \quad (19)$$

Here $\ddot{R}$ is the resistance of each considered layer in the cell that is calculated based on thickness and resistivity of each layer [48]:

$$\ddot{R}_i = \delta_i \rho_i \quad (20)$$

Here, thickness and resistivity of anode, cathode, interconnect, and electrolyte can be considered even though it is known that the highest resistance belongs to electrolyte and the rest in general is neglected. Concentration overpotentials are related to mass transfer limitations on electrodes as well species concentrations. Due to change in concentration of species resulted in current passing through the electrodes a voltage change is also present. The simplest way to determine concentration losses is by introducing limiting current density that is based on mass transfer, electrochemistry, and boundary layer theory:

$$\frac{j_L}{ZF} = -D\frac{c_o}{\delta} \quad (21)$$

where D is diffusivity diameter and c^0 is species concentration and the concentration overpotential is:

$$E_{con} = \frac{RT}{zF} \ln\left(1 - \frac{j}{j_L}\right) \quad (22)$$

There are several other formulated and correlated definitions for concentration overpotentials that can be utilized based on the work being conducted. Finally, efficiency of the cell can be written as the ratio of useful outputs from the cathode to consumed power and required heating. This can be basically determined by writing the energy balance of the system:

$$\dot{Q} - \dot{W} = \sum_{P} \dot{N}_i \left[\Delta H_{f_i}^0 + H_i(T_p) - H_i^0\right] - \sum_{R} \dot{N}_i \left[\Delta H_{f_i}^0 + H_i(T_R) - H_i^0\right] \quad (23)$$

Where $\Delta H_{f_i}^0$ is enthalpy of formation for each reactant or product while the term $H_i(T_R) - H_i^0$ corresponds to the sensible enthalpy. The efficiency of the cell is:

$$\eta_{cell} = \frac{LHV_{CO}\dot{n}_{co,2} + LHV_{H_2}\dot{n}_{H_2,2}}{\dot{Q} + E_{tot}JA_{cell}N_{cell}} \quad (24)$$

Where *LHV* is the lower heating value of the corresponding fuel, A_{cell} is cell area and N_{cell} is number of cells used. Molar flow rates at the exit are calculated based on either a known ionic transfer of oxygen or a known inlet molar flow rate. The H_2/CO ratio is also an important aspect to evaluate its possibility to produce chemical feedstock. Feedstock conversion factor is the rate of converted H_2O/CO_2 to H_2/CO:

$$\psi = \frac{\dot{n}_{in}(y_{0,H2O} + y_{0,CO2}) - \dot{n}_{out}(y_{2,H2O} + y_{2,CO2})}{\dot{n}_{in}(y_{0,H2O} + y_{0,CO2})} \quad (25)$$

It is also possible to simply calculate overpotentials with a term called area specific resistance (ASR) as a function of cell temperature and pressure:

$$E_{tot} = E_N + ASR(T, P) \quad (26)$$

$$ASR = 34.22 \exp(T_{cell} - 273.15) \exp(-0.0217 P_{cell}) \quad (27)$$

2.2 Multi-dimensional modeling

COMSOL is utilized for the multi-dimensional modelling work. There are not many available works published or presented for modelling aspects of gas mixtures through a co-electrolysis cell, however, there are many represented for simple H_2 SOEC at cell level as mentioned in the literature review of this work. Therefore, available works for H_2-SOEC cell configurations are taken into account to validate the modelling results. In addition, in order to decrease the solution time and complexity, it is aimed to decrease the modelling space into 2D. The cell model that is introduced in the zero-dimensional model has been utilized for the multi-dimensional model for a planar cell.

The planar cell configuration geometry is represented in Figure 1. An 8x8 cm cell is designed with anode, electrolyte and cathode while a surface current collector is considered at the upper surface of the cathode. The gas domain is located at the top of the cathode layer with various channels to collect the generated gas. Geometry and physical parameters of the cell that is fed into COMSOL. Channel width and length, gas domain height, cell depth and thickness of electrode/electrolyte layers are provided based on available cell structures. In the case of a cathode supported cell the cathode is three times thicker than anode and electrolyte. Instead of utilizing the material library of COMSOL, some certain basic physical parameters are considered for common electrode/electrolyte materials such as permeability and porosity of electrodes and conductivity of electrolyte.

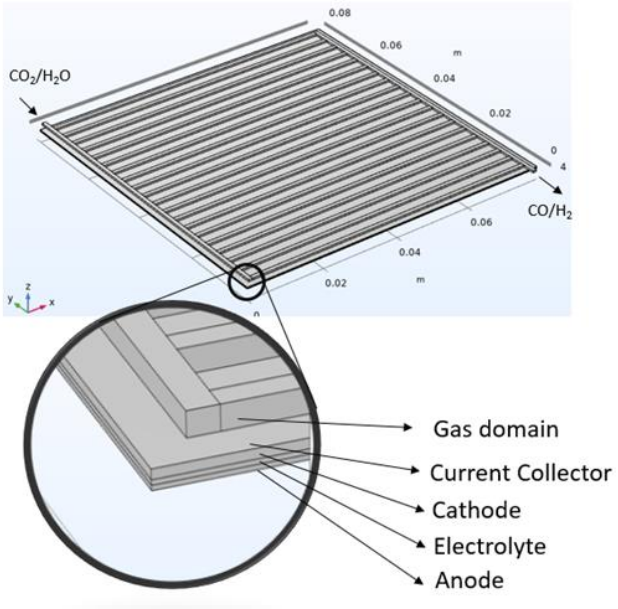

Figure 1. Planar cell configuration

To prevent solution complexity, dimensions of the cell is decreased to 2D. Meshing of the geometry is kept simple and free triangular shaped meshes are considered for all layers of the cell as in Figure 2. No slip condition is assigned for the boundary of the gas domain and the number of boundary layers is taken as four. Four study trees are formed for the analysis of the planar cell design in which the first two considers secondary current distribution alone, the third one integrates Brinkmann equations to take into account the porous media flow while the last one considers Multiphysics of reacting flow and the predefined tools together.

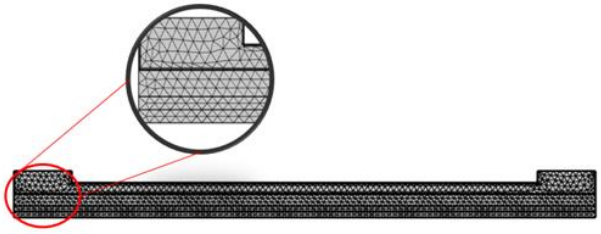

Figure 2. Meshing of the 2D model for co-electrolysis

The momentum, energy and mass equations are dictated by COMSOL through the solution where data manipulation is only required to feed two different gas species. Energy conservation equation becomes challenging when radiative heat transfer is included, therefore it is generally neglected. The energy conservation should be considered as conduction heat transfer in solid structures and convective heat transfer in gas channels. Governing equations for momentum conservation is included for both cathode, anode and channels separately. The general Momentum equation in the gas channels is:

$$\rho\frac{\partial u}{\partial t}+\rho u\cdot\nabla u=-\nabla p+\nabla \cdot\left[\mu(Vu+(Vu)^{T})-\frac{2}{3}\mu\nabla\cdot u\right]+Q_u \quad (28)$$

and

$$\frac{\partial \rho}{\partial t}+\nabla\cdot(\rho u)=Q_M \quad (29)$$

According to Darcy's law Q_u is equal to $-(\varepsilon\mu/K)\vec{v}$ and Q_M is related to current density, where K is permeability and μ is dynamic viscosity.

3 Results and discussion

Results of the zero-dimensional model is provided for thermal and efficiency analysis with validation. Based on the model, effects of temperature, pressure, current density and other major parameters are investigated in order to provide adequate amount of information on optimal operation of the considered cell. Validation of the model is conducted by comparing the cell outlet gas stream's molar fractions at different ionic currents as in Figure 3. The molar fractions of the model and Stoot et al's work are well aligned [5].

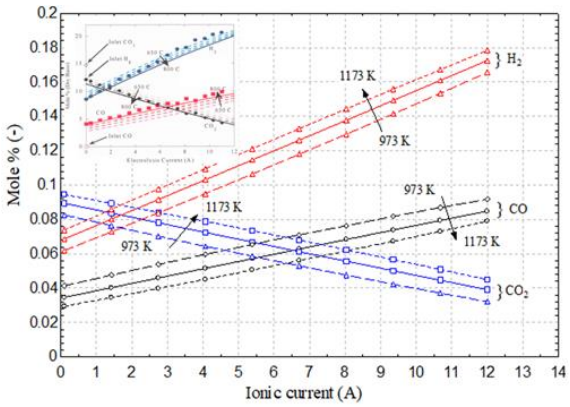

Figure 3. Validation of the existing model with the experimental results represented in [5]

Current density is one of the most influential parameters that effects cell performances overall. Therefore, its variation is critical to figure out certain optimal conditions through the cell when thermodynamic modeling is applied. Higher current density and lower temperature operation expectedly have the negative effect on the cell performance as in Figure 4.

Figure 5 represents effects of current density and temperature change on overpotentials and cell efficiency. An optimal current density is available which is slight lower than 1000 A/m^2 to provide low overpotentials and higher efficiency. Maximum reachable cell efficiency in this case is abo 75%. The comparatively low current density requirement potentially carries the disadvantage of higher space requirements plus extra materials use for the same number of products compared to legacy systems that produce hydrogen. However, in this case co-electrolysis is only possible with high temperature electrolysers and making such a comparison might stand unnecessary. Here, the main motivation is to keep the efficiency of the process as high as possible and capture CO_2.

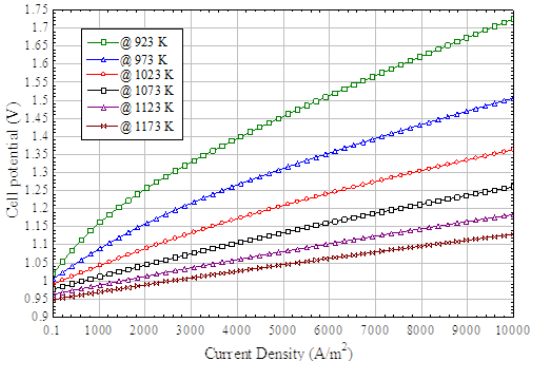

Figure 4. Effect of current density and temperature on cell potential

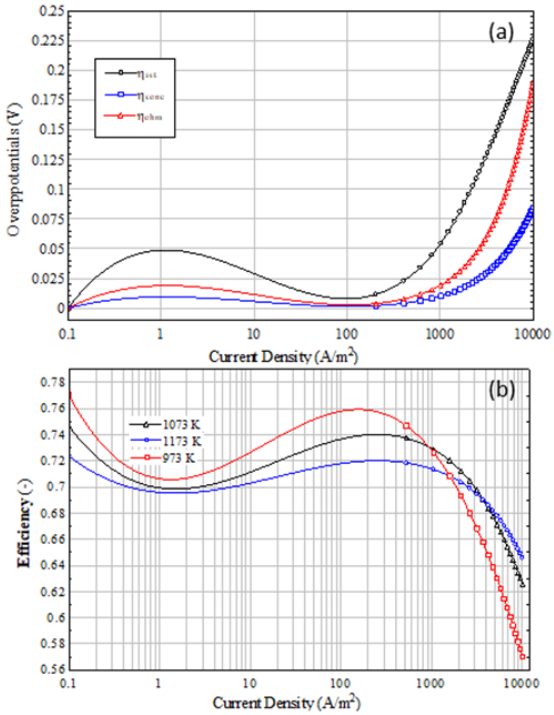

Figure 5. Trend of (a) cell overpotentials and (b) cell efficiency at various current densities

Figure 6 represents result for the model that is based on area specific resistances. Effects of cell temperature and pressure is investigated in this case that higher pressures cause a decrease in cell efficiency up to 1.5 MPa while a significant increase is observed after this value where there should be an upper limit for safer operation, while higher temperature tends to increase the cell efficiency. Higher pressure operation for SOFCs have long been discussed yet shows many added challenges to already complex high temperature operation. However, for the co-electrolysis case, including the thermochemistry of CO_2 presence and CO production equilibrium constant is favoured at a certain pressure range that should be noted down for future investigations.

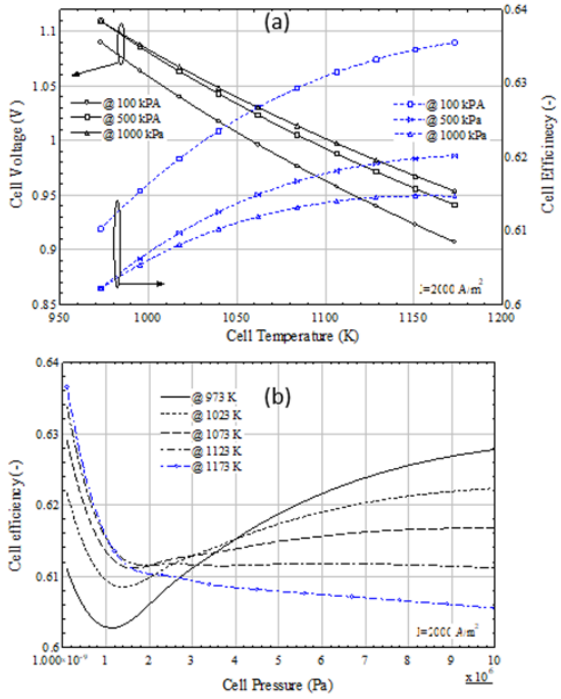

Figure 6. Effects of combined cell temperature and pressure on (a) cell voltage and (b) cell efficiency

Considering cell configurations, SOECs can be planar, tubular, or flat tubular. Early SOEC systems used tubular cells as their geometry. When compared to planar configurations, higher mechanical and thermal stability can be achieved with tubular configurations. Sealing of the cell is also much easier in tubular configurations than that of flat-plate configurations as the sealing area is significantly reduced. However, planar designs are still being widely adopted due to their much shorter current collection paths and significantly higher volumetric density. Here, for a micro-scale SOEC electrode model ion/electronic charge transport, mass, momentum, and energy conservation equations should be considered.

Initially the feed stream is considered as water into the cell to observe validity of the model. However, significant amount of meshing in very high number of channels considered in the cell mainly either failed for evaluation or takes significant amount of time for solution, which might be misleading and unnecessary. Therefore, number of channels are decreased to an acceptable level. Electrolyte potential provides a practical range of open cell voltage for the cell with considered overpotentials utilized through the study tree. Figure 7 demonstrates distribution of velocity and electrolyte potential, as well as molar concentrations of water and hydrogen on the cathodic surface. Water is completely consumed and converted into hydrogen as its molarity significantly decreased through the cell inlet/outlet while the opposite occurs for hydrogen.

The 3D model for H_2-SOEC is than configured into a 2D model for decreased solution complexity in which it is obvious that 3D model does not provide further insight for what was intended to investigate in the part of the study. For the cathodic gas system Kinetic and Brokaw theories are selected for gas diffusivity and viscosity models for CO, CO_2, H_2 and H_2O system. The oxygen ions transferred to anode has been excluded from the 2D analysis to focus on the cathodic distributions. Secondary current distribution tool is used to model the voltage-current characteristics on the cell by assigning structures for cell layers with geometric and physical parameters. Low velocity flow in porous media is defined using the Brinkmann equations as a ready to use tool in COMSOL. Finally, the Transport of Concentrated species (TCS) tool is utilized to investigate the flow and distribution of substances at the cathode side. Maxwell-Stefan diffusion model is used in this tool while it also considers transport in porous media and migration in an electric field. All substances are assumed as ideal gas and remaining of all calculations are based on ideal gas law.

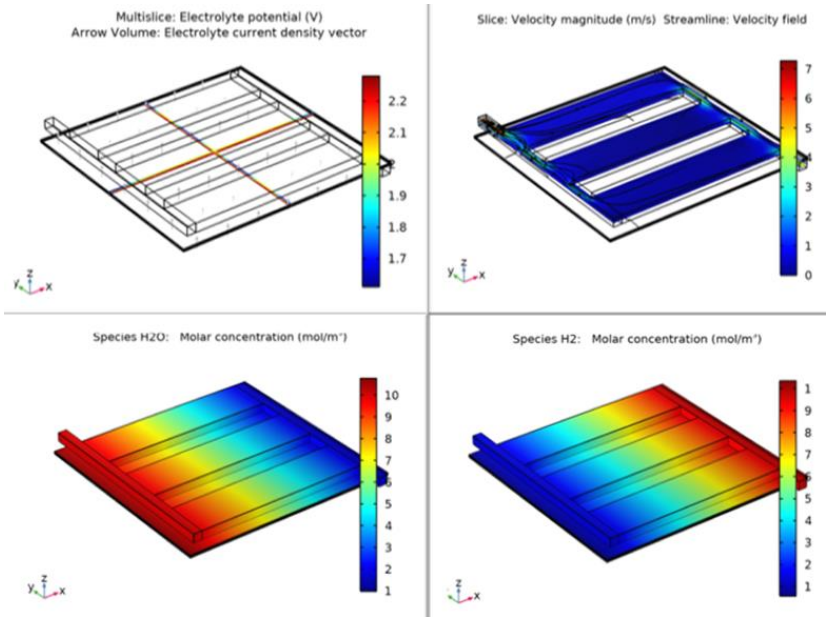

Figure 7. Electrolyte potential, velocity field and molar concentrations for the reference 3D H_2 – SOEC model

Figure 8 represents the electrolyte potential, electrode current density and velocity distributions through the 2D planar cell design. Distributions are well aligned with the 3D design for water electrolysis in co-electrolysis mode. In this case the cell potential is above 1.3V and up to 1.6V, which is expected for the cell in co-electrolysis mode. Current density of the cell is limited to 0.1 A/cm^2 for this case to prevent solution complexities at high current densities.

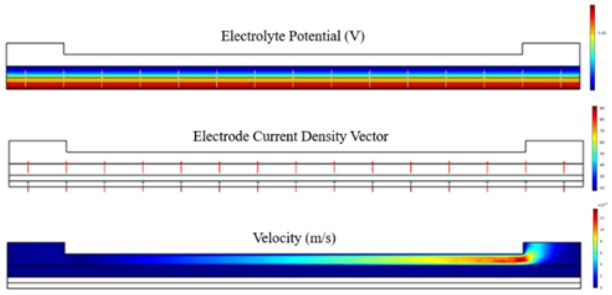

Figure 8. Electrolyte potential, electrode current density and velocity distributions through the 2D planar cell design

Under stoichiometry, the distributions of all chemical species at the cathode side are evaluated. Lower current densities results in lower product conversions and for the case of 0.01 A/cm^2, 20% fuel utilization can be accomplished while it can be increased up to 60% at higher current densities as recommended in the zero-dimensional model, suggesting that the multi-dimensional model provides acceptable analysis results in parallel to the zero-dimensional model with further details, which is based on experimental results. In this case it may be more convenient to use modelling tools in order to investigate thermal/efficiency characteristics of such cell to create a base for experimentation and utilization of such systems. However, the zero-dimensional model considers basic chemical reactions without considering detailed interactions between reacting substances through the cell and may fall short fall to provide a better insight. Therefore, utilizing tools in COMSOL provides a better understanding on at least the behavior of substances through a porous media. This alone considers the effect of electrolysis process on the conversion of the feed while the reverse water shift reaction distribution is not taken into account, however, it can be seen that a significant amount of CO production is already accomplished at the inlet. The zero-dimensional model shows that the molar composition of the cell inlet already accomplishes most of the CO production through the RGWS reaction.

4 Conclusions

SOEC technology has long been under research as a reverse SOFC while there have been new initiatives to utilize these cells in power generation industry for energy storage purposes. SOEC technology is an efficient alternative to conventional electrolysis while it also can be used for syngas production due to its high temperature operation. In this research co-electrolysis of CO_2 and steam, two of the common waste from industry are utilized for recovery and capture of CO_2 to produce syngas, which can make a significant contribution to short/near term zero emission targets. A zero-dimensional model is developed to investigate efficiency aspect of a single planar cell design followed by multi-dimensional analysis of the same cell using COMSOL platform, where COMSOL provides detailed information and a better understanding of the species distributions by considering many more theoretical tools and Multiphysics modelling. The fuel utilization factor may be as high as 60% under similar current density-voltage conditions while the species distribution results show that the H_2 to CO ratio is at an acceptable range that they can be further utilized for methane or liquid fuel synthesis. COMSOL can be used to expand the studies not only for single cell design but also at stack level to understand thermo mechanical trends through operation to understand the causes of degradation and system lifetime.

Acknowledgment

Author acknowledges Imperial College London's Department of Earth Sciences for allowing the author to use the COMSOL workstation.

Conflict of interest

The author declares no conflict of interest.

Similarity rate (iThenticate): 15%

References

[1] A. Körner, C. Tam, S. Bennett and J. Gagné, Technology roadmap-hydrogen and fuel cells. Technical Annex for International Energy Agency (IEA), page 3-7, Paris, France, 29 June 2015.

[2] B. Lei, B. Samir and T. Enrico. Steam electrolysis by solid oxide electrolysis cells (SOECs) with proton-conducting oxides. Chemical Society Reviews, 43(24), 8255-8270, 2014. https://doi.org/10.1039/C4CS00194J

[3] S. D. Ebbesen, R. Knibbe and M. Mogensen, Co-electrolysis of steam and carbon dioxide in solid oxide cells. Journal of the Electrochemical Society, 159(8), F482, 2012. https://doi.org/10.1149/2.076208jes

[4] S. D. Ebbesen, C. Graves and M Mogensen, Production of synthetic fuels by co-electrolysis of steam and carbon dioxide. International Journal of Green Energy, 6(6), 646-660, 2009. https://doi.org/10.1080/15435070903372577

[5] C. M. Stoots, J. E. O'brien, J. S. Herring and J. J Hartvingsen, Syngas production via high-temperature coelectrolysis of steam and carbon dioxide. Journal of fuel cell science and technology, 6, 1, 2009.

[6] S. D. Ebbesen, C. Graves, A. Hauch, S. H. Hensen and M. Mogensen, Poisoning of solid oxide electrolysis cells by impurities. Journal of the Electrochemical Society, 157(10), B1419, 2010. https://doi.org/https://doi.org/10.1149/1.3464804

[7] N. Q. Minh and M. Mogensen. Reversible solid oxide fuel cell technology for green fuel and power

production. The electrochemical Society Interface, 22(4), 55, 2013. https://doi.org/https://doi.org/10.1149/2.F05134if

[8] Y. Zheng, J. Wang, B. Yu, W. Zhang, J. Chen, J. Qiao and J. Zhang, A review of high temperature co-electrolysis of H_2O and CO_2 to produce sustainable fuels using solid oxide electrolysis cells (SOECs): advanced materials and technology. Chemical Society Reviews, 46(5), 1427-1463, 2017. https://doi.org/10.1039/C6CS00403B

[9] T. Wei, P. Singh, Y. Gong, J. B. Goodenough, Y. Huang and K. Huang, Sr 3− 3x Na 3x Si 3 O 9− 1.5 x (x= 0.45) as a superior solid oxide-ion electrolyte for intermediate temperature-solid oxide fuel cells. Energy & Environmental Science, 7(5), 1680-1684, 2014. https://doi.org/10.1039/C3EE43730B

[10] Y. Wang, T. Liu, S. Fang and F. Chen, Syngas production on a symmetrical solid oxide H2O/CO2 co-electrolysis cell with Sr2Fe1. 5Mo0. 5O6–Sm0. 2Ce0. 8O1. 9 electrodes. Journal of Power Sources, 305, 240-248, 2016. https://doi.org/10.1016/j.jpowsour.2015.11.097

[11] Q. Liu, C. Yang, X. Dong and F. Chen. Perovskite Sr2Fe1. 5Mo0. 5O6− δ as electrode materials for symmetrical solid oxide electrolysis cells. International Journal of Hydrogen Energy, 35(19), 10039-10044, 2010. https://doi.org/10.1016/j.ijhydene.2010.08.016

[12] T. Chen, M. Liu, Y. Zhou, X. Ye and Z. Zhan, High performance of intermediate temperature solid oxide electrolysis cells using Nd2NiO4+ δ impregnated scandia stabilized zirconia oxygen electrode. Journal of Power Sources, 276, 1-6, 2015. https://doi.org/10.1016/j.jpowsour.2014.11.042

[13] J. Li, C. Zhong, X. Meng, H. Wu, H. Nie, Z. Zhan and S. Wang, Sr2Fe1. 5Mo0. 5O6–δ–Zr0. 84Y0. 16O2–δ Materials as Oxygen Electrodes for Solid Oxide Electrolysis Cells. Fuel Cells, 14(6), 1046-1049, 2014. https://doi.org/10.1002/fuce.201400021

[14] C. Graves, S. D. Ebbesen and M. Mogensen, Co-electrolysis of CO2 and H2O in solid oxide cells: performance and durability. Solid State Ionics, 192(1), 398-403, 2011. https://doi.org/10.1016/j.ssi.2010.06.014

[15] W. Li, H. Wang, Y. Shi and N. Cai, Performance and methane production characteristics of H2O–CO2 co-electrolysis in solid oxide electrolysis cells. International journal of hydrogen energy, 38(25), 11104-11109, 2013. https://doi.org/10.1016/j.ijhydene.2013.01.008

[16] C. Stoots., J. O'Brien and J. Hartvigsen, Results of recent high temperature coelectrolysis studies at the Idaho National Laboratory. International Journal of Hydrogen Energy, 34(9), 4208-4215, 2009. https://doi.org/10.1016/j.ijhydene.2008.08.029

[17] K. Chen, S. Liu, N. Ai, M. Koyama and S. P. Jiang, Why solid oxide cells can be reversibly operated in solid oxide electrolysis cell and fuel cell modes?. Physical Chemistry Chemical Physics, 17(46), 31308-31315, 2015. https://doi.org/10.1039/C5CP05065K

[18] C. Graves, S. D. Ebbesen, S. H. Jensen, S. B. Simonsen and M. Mogensen, Eliminating degradation in solid oxide electrochemical cells by reversible operation. Nature materials, 14(2), 239-244, 2015. https://doi.org/10.1038/NMAT4165

[19] G. A. Hughes, K. Yakal-Kremski and S. A. Barnett, Life testing of LSM–YSZ composite electrodes under reversing-current operation. Physical Chemistry Chemical Physics, 15(40), 17257-17262, 2013. https://doi.org/10.1039/C3CP52973H

[20] A. Hauch, S. D. Ebbesen, S. H. Jensen and M. Mogensen, Solid oxide electrolysis cells: Microstructure and degradation of the Ni/yttria-stabilized zirconia electrode. Journal of the Electrochemical Society, 155(11), B1184, 2008. https://doi.org/10.1149/1.2967331

[21] A. Hauch, S. H. Jensen, J. B. Bilde-Sørensen and M. Mogensen, Silica segregation in the Ni∕YSZ electrode. Journal of the Electrochemical Society, 154(7), A619, 2007. https://doi.org/10.1149/1.2733861

[22] M. A. Laguna-Bercero, J. A. Kilner and S. J. Skinner, Development of oxygen electrodes for reversible solid oxide fuel cells with scandia stabilized zirconia electrolytes. Solid State Ionics, 192(1), 501-504, 2011 https://doi.org/10.1016/j.ssi.2010.01.003.

[23] W. Wang, Y. Huang, S. Jung, J. M. Vohs and R. J. Gorte, A comparison of LSM, LSF, and LSCo for solid oxide electrolyzer anodes. Journal of the Electrochemical Society, 153(11), A2066, 2006 https://doi.org/10.1149/1.2345583.

[24] P. Hjalmarsson, X. Sun, Y. L. Liu and M. Chen, Influence of the oxygen electrode and inter-diffusion barrier on the degradation of solid oxide electrolysis cells. Journal of power sources, 223, 349-357, 2013. https://doi.org/10.1016/j.jpowsour.2012.08.063

[25] K. Chen and N. Ai, Development of (Gd, Ce) O2-impregnated (La, Sr) MnO3 anodes of high temperature solid oxide electrolysis cells. Journal of the Electrochemical Society, 157(11), P89, 2010. https://doi.org/10.1149/1.3481436

[26] B. Yu, W. Zhang, J. Xu, J. Chen, X. Luo and K. Stephan, Preparation and electrochemical behavior of dense YSZ film for SOEC. International journal of hydrogen energy, 37(17), 12074-12080, 2010. https://doi.org/10.1016/j.ijhydene.2012.05.063

[27] W. Zhang, B. Yu and J. Xu, Investigation of single SOEC with BSCF anode and SDC barrier layer. International journal of hydrogen energy, 37(1), 837-842, 2012. https://doi.org/10.1016/j.ijhydene.2011.04.049

[28] R. Xing, Y. Wang, Y. Zhu, S. Liu and C. Jin, Co-electrolysis of steam and CO2 in a solid oxide electrolysis cell with La0. 75Sr0. 25Cr0. 5Mn0. 5O3− δ–Cu ceramic composite electrode. Journal of Power Sources, 274, 260-264, 2015. https://doi.org/10.1016/j.jpowsour.2014.10.066

[29] T. Chen, M. Liu, C. Yuan, Y. Zhou, X. Ye, Z. Zhan, C. Xia and S. Wang, High performance of intermediate temperature solid oxide electrolysis cells using

Nd2NiO4+ δ impregnated scandia stabilized zirconia oxygen electrode. Journal of Power Sources, 276, 1-6, 2015. https://doi.org/10.1016/j.jpowsour.2014.11.042

[30] T. Ogier, J. M. Bassat, F. Mauvy, S. Fourcade, J. C. Grenier, K. Couturier, M. Petitjean and J. Mougin, Enhanced performances of structured oxygen electrodes for high temperature steam electrolysis. Fuel Cells, 13(4), 536-541, 2013. https://doi.org/10.1002/fuce.201200201

[31] J. Schefold, A. Brisse and F. Tietz, Nine thousand hours of operation of a solid oxide cell in steam electrolysis mode. Journal of the Electrochemical Society, 159(2), A137, 2011. https://doi.org/10.1149/2.076202jes

[32] P. Moçoteguy and A. Brisse, A review and comprehensive analysis of degradation mechanisms of solid oxide electrolysis cells. International journal of hydrogen energy, 38(36), 15887-15902, 2013. https://doi.org/10.1016/j.ijhydene.2013.09.045

[33] M. S. Sohal, J. E. O'Brien, C. M. Stoots, V. L. Sharma, B. Yildiz and A. Virkar, Degradation issues in solid oxide cells during high temperature electrolysis. Journal of Fuel Cell Science and Technology, 9(1), 2012. https://doi.org/10.1115/1.4003787

[34] G. L. Hawkes, J. E. O'Brien, C. M. Stoots and R. Jones, 3D CFD Model of High Temperature H2O/CO2 Co-Electrolysis. ANS Summer Meeting, Boston, June 24, 2007.https://www2.ans.org/meetings/docs/2007/am2007-official.pdf

[35] J. E. O'Brien, M. G. McKellar, C. Stoots, J. S. Herring and G. L. Hawkes, Parametric study of large-scale production of syngas via high-temperature co-electrolysis. International Journal of Hydrogen Energy, 34(9), 4216-4226, 2009. https://doi.org/10.1016/j.ijhydene.2008.12.021

[36] M. G. McKellar, J. E. O'Brien, C. M. Stoots and G. L. Hawkes, Process Model for the Production of Syngas Via High Temperature Co-Electrolysis. In ASME International Mechanical Engineering Congress and Exposition, vol. 43009, pp. 691-699, 2007. https://doi.org/10.1115/IMECE2007-43658

[37] Z. Zhan, W. Kobsiriphat, J. R. Wilson, M. Pillai, I. Kim and S. A. Barnett, Syngas production by coelectrolysis of CO2/H2O: the basis for a renewable energy cycle. Energy & Fuels, 23(6), 3089-3096, 2009. https://doi.org/10.1021/ef900111f

[38] C. R. Graves, Recycling co2 into sustainable hydrocarbon fuels: Electrolysis of co2 and h2o. Doctoral dissertation, Columbia University, USA, 2010.

[39] Y. Wang, T. Liu, S. Fang, G. Xiao, H. Wang and F. Chen, A novel clean and effective syngas production system based on partial oxidation of methane assisted solid oxide co-electrolysis process. Journal of Power Sources, 277, 261-267, 2015. https://doi.org/10.1016/j.jpowsour.2014.11.092

[40] N. Q. Minh and M. B. Mogensen, Reversible solid oxide fuel cell technology for green fuel and power production. The electrochemical Society Interface, 22(4), 55, 2013. https://doi.org/10.1149/2.F05134if

[41] Y. Wang, Y. Du, M. Ni, R. Zhan, Q. Du and K. Jiao, Three-dimensional modeling of flow field optimization for co-electrolysis solid oxide electrolysis cell. Applied Thermal Engineering, 172, 114959, 2020. https://doi.org/10.1016/j.applthermaleng.2020.114959

[42] Y. Chen, Y. Luo, Y. Shi and N. Cai, Theoretical modeling of a pressurized tubular reversible solid oxide cell for methane production by co-electrolysis. Applied Energy, 268, 114927, 2020. https://doi.org/10.1016/j.apenergy.2020.114927

[43] D. Y. Lee, M. T. Mehran, J. Kim, S. Kim, S. B. Lee, R. H. Song, E. Y. Ko, J. E. Hong, J. Y. Huh and T. H. Lim, Scaling up syngas production with controllable H2/CO ratio in a highly efficient, compact, and durable solid oxide coelectrolysis cell unit-bundle. Applied Energy, 257, 114036, 2020. https://doi.org/10.1016/j.apenergy.2019.114036

[44] E. P. Reznicek and R. J. Braun, Reversible solid oxide cell systems for integration with natural gas pipeline and carbon capture infrastructure for grid energy management. Applied Energy, 259, 114118, 2020. https://doi.org/10.1016/j.apenergy.2019.114118

[45] A. P. Kulkarni, T. Hos, M. V. Landau, D. Fini, S. Giddey and M. Herskowitz, Techno-economic analysis of a sustainable process for converting CO 2 and H 2 O to feedstock for fuels and chemicals. Sustainable Energy & Fuels, 5(2), 486-500, 2021. https://doi.org/10.1039/D0SE01125H

[46] C. O. Colpan, F. Hamdullahpur and I. Dincer, Heat-up and start-up modeling of direct internal reforming solid oxide fuel cells. Journal of Power Sources, 195(11), 3579-3589, 2010. https://doi.org/10.1016/j.jpowsour.2009.12.021

[47] C. M. Stoots, J. E. O'Brien, J. Herring and J. J. Hartvigsen, Syngas production via high-temperature coelectrolysis of steam and carbon dioxide, J. Fuel Cell Sci. Technol, 6(1): 011014, 2009. https://doi.org/10.1115/1.2971061

[48] J. P. Stempien, O. L. Ding, Q. Sun and S. H. Chan, Energy and exergy analysis of Solid Oxide Electrolyser Cell (SOEC) working as a CO2 mitigation device. International Journal of Hydrogen Energy, 37(19), 14518-14527, 2012. https://doi.org/10.1016/j.ijhydene.2012.07.065